

Julolidine-Based Small Molecular Probes for Fluorescence Imaging of RNA in Live Cells

Iswar Chandra Mondal,^a Priya Rawat,^b Maksym Galkin,^c Snata Deka,^a Anirban Karmakar,^c Prosenjit Mondal,^{*b} and Subrata Ghosh^{*a}

Table of Contents:

S. No.	Contents	Page No.
1.	Experimental Procedures	1
2.	Optical Responses of the Probes	2-3
3.	Solvatochromic Study	4-7
3	Calculation of Extinction coefficients	8-9
5	Calculation of detection limit	11
6	Optical response of probe with other Analytes	11
7	Effect of pH and Cytotoxicity assay	14-15
8	Quantification of the photostability	16
9	Synthetic protocols, structural characterization of the precursor and the probes using ¹ H/ ¹³ C NMR and MS of the synthesized compounds.	16-30
10	SCXRD analysis	30-32
11	References	32

Experimental Procedures:

Calculation of extinction coefficient: The values of the extinction coefficient were evaluated for all the probes in the presence and absence of RNA. Absorption spectra were obtained by titrating 1 mL of PBS with 0 – 12 μ M concentration of probe and the value of the extinction coefficient was evaluated as the slope of the plot between absorption maxima vs concentrations. Similarly, absorption spectra of various concentration (0 – 12 μ M) of probe SEZ-JLD was recorded in the presence of 1 mg/mL of RNA solution and the extinction coefficient value was calculated from the slope of absorbance vs concentration graph. The plot between absorption maxima vs concentration in the absence and presence of RNA for probe SEZ-JLD is illustrated in Fig. S7 and S8 respectively.

Solvatochromic study: DCM, ACN, H₂O, MeOH, and DMSO were used as solvents of different polarities for this study. The experimental temperature was ~20-25 °C. Here, the stock solution of the dyes was prepared in DMSO.

Effect of pH on the optical response of probe-RNA complex: RNA solution (1 mg/mL RNA) was prepared in PBS at different pH (pH 4-10). Next, 5 μ M of respective dyes were added to it and the fluorescence responses were recorded at a temperature of ~20-25 °C.

Determination of the experimental limit of detection: Experimental limit of detection was calculated using the reported procedure.¹ RNA concentration at which emission enhancement for the probe was more than 10% of their initial emission intensity was considered as the detection limit.

Relative Quantum yield calculation: Relative quantum yield of all the probes was determined using Rhodamine B ($\phi_R = 0.68$, in Ethanol) as the standard (on SHIMADZU UV-2450 spectrophotometer and Agilent Cary Eclipse fluorescence spectrometer, slit widths of 1/1 for absorption and 5/5 for emission respectively) using equation:²

$$\phi_S = \phi_R \left(\frac{A_R}{A_S} \right) \left(\frac{D_S}{D_R} \right) \left[\frac{n_S}{n_R} \right]^2$$

Where ϕ_S and ϕ_R ; the quantum yields of the sample and the reference, A_S and A_R ; absorbance of the sample and the reference. D_S and D_R ; the areas of emission while n_S and n_R ; the refractive indices of the sample (corrected to be PBS) and reference solutions (corrected to be ethanol) respectively.² For this calculation, we made the absorption intensity of sample and reference almost equal and then excited the sample and reference at their individual absorption maximum wavelength to obtain the emission spectra.

Table S1: Optical properties of OX-JLD, BTZ-JLD, and SEZ-JLD in different solvents.

OX-JLD	λ_{\max} Abs (nm)	λ_{\max} Em (nm)	Stokes Shift (nm)	Molar Absorptivity ($M^{-1}cm^{-1}$)
H ₂ O	524	575	51	2.5×10^4
DCM	554	577	23	4.6×10^4
ACN	532	580	48	2.7×10^4
MeOH	530	574	44	2.6×10^4
DMSO	530	588	58	2.2×10^4

BTZ-JLD	λ_{\max} Abs (nm)	λ_{\max} Em (nm)	Stokes Shift (nm)	Molar Absorptivity ($M^{-1} cm^{-1}$)
H ₂ O	554	616	62	2.6×10^4
DCM	590	618	28	4.8×10^4
ACN	564	620	56	3.2×10^4
MeOH	564	612	48	3.2×10^4
DMSO	564	627	63	2.6×10^4

SEZ-JLD	λ_{\max} Abs (nm)	λ_{\max} Em (nm)	Stokes Shift (nm)	Molar Absorptivity ($M^{-1}cm^{-1}$)
H ₂ O	570	620	50	2.5×10^4
DCM	600	625	25	4.9×10^4
ACN	574	624	50	3.1×10^4
MeOH	574	621	47	3.1×10^4
DMSO	574	629	55	2.5×10^4

Table S2: Lifetime of SEZ-JLD in the presence of RNA and in a medium with different viscosity.

Probe	τ_1 (ns)	τ_2 (ns)	χ^2	Average lifetime (ns)
SEZ-JLD+RNA (574 nm)	1.11	3.08	0.90	2.26
20% Glycerol in water	0.13	-	1.07	0.13
80% Glycerol in water	0.28	-	0.86	0.28
Glycerol	0.5	-	1.07	0.5

Table S3: Optical parameters of SEZ-JLD in the presence of RNA

Probe	Extinction Coefficient ^a (ϵ) ($M^{-1} cm^{-1}$) (Approx.)	Quantum Yield ^b (Φ)	Brightness ^c (In PBS) ($\epsilon \times \Phi$) (Approx.) ($M^{-1} cm^{-1}$)
SEZ-JLD	17800	0.007 $\lambda_{\text{abs max}}$ (SEZ-JLD+PBS) = 571 nm $\lambda_{\text{abs max}}$ (RhB) = 545 nm	124
SEZ-JLD+RNA	26500	0.34 $\lambda_{\text{abs max}}$ (SEZ-JLD+RNA) = 605 nm $\lambda_{\text{abs max}}$ (RhB) = 545 nm	9010

^a extinction coefficient, ^b quantum yield, ^c brightness

Table S4: Relative Quantum Yield of OX-JLD and BTZ-JLD with and without RNA.

Probe	OX-JLD+PBS	OXJLD+RNA	BTZ-JLD+PBS	BTZ-JLD+RNA
Quantum Yield	0.0041	0.41	0.0019	0.43

** Rhodamine B was used as reference dye.*

Table S5: Relative Quantum yield of SEZ-JLD in different solvents.

SEZ-JLD	H ₂ O	DCM	ACN	MeOH	DMSO
Quantum Yield	0.0020	0.0036	0.0017	0.0029	.0120

** Rhodamine B was used as reference dye.*

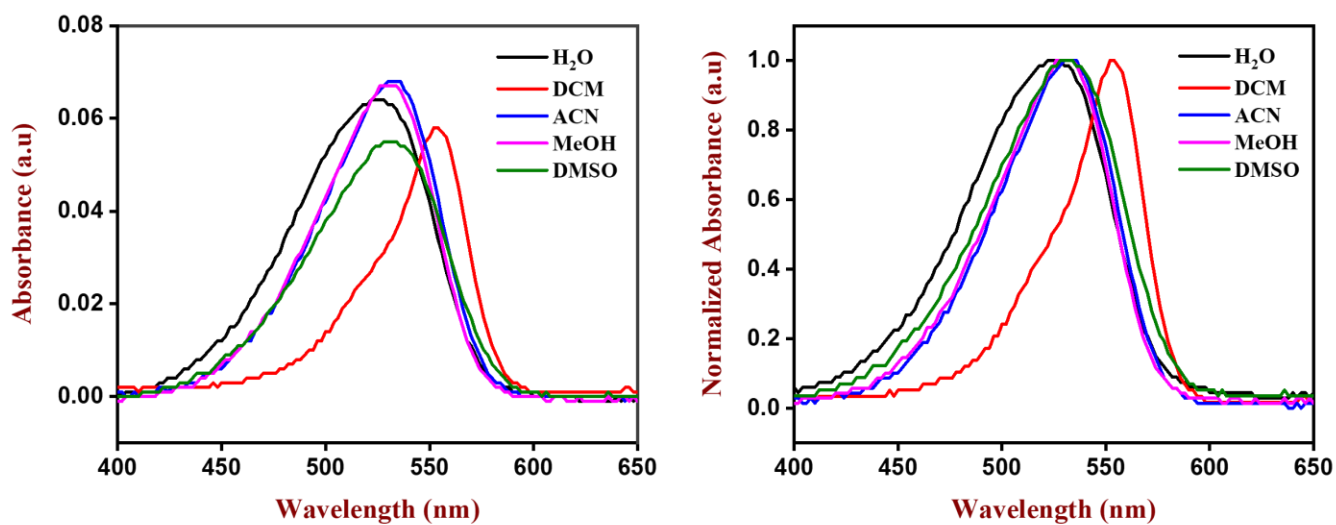


Figure S1: Absorption spectra and their normalized profiles of OX-JLD in different solvents

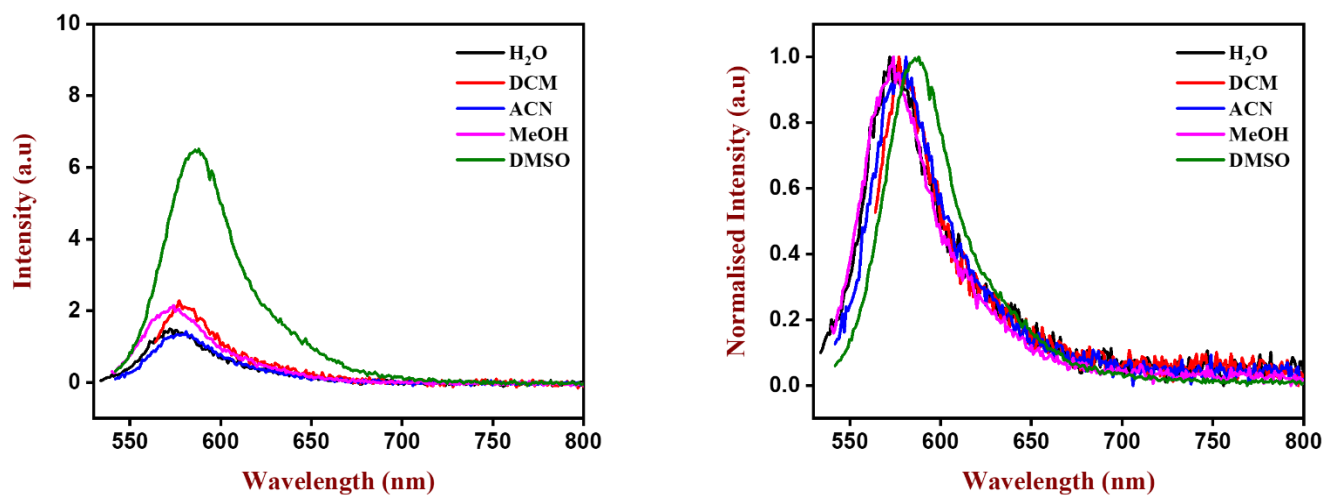


Figure S2: Emission spectra and normalized spectra of OX-JLD in different solvents

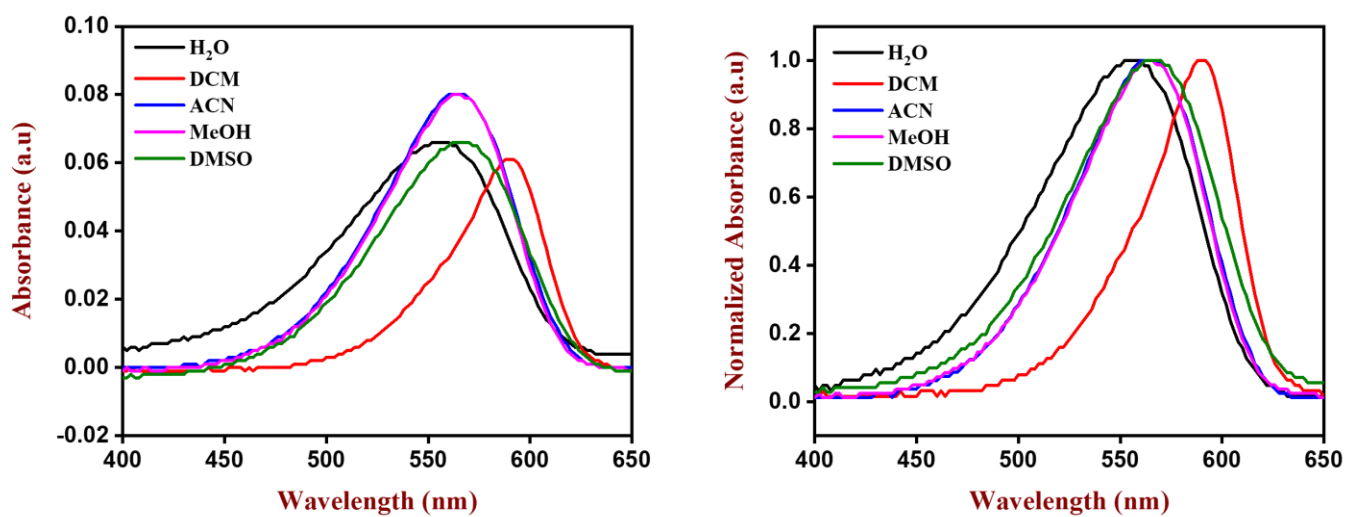


Figure S3: Absorption spectra and their normalized spectra of BTZ-JLD in different solvents

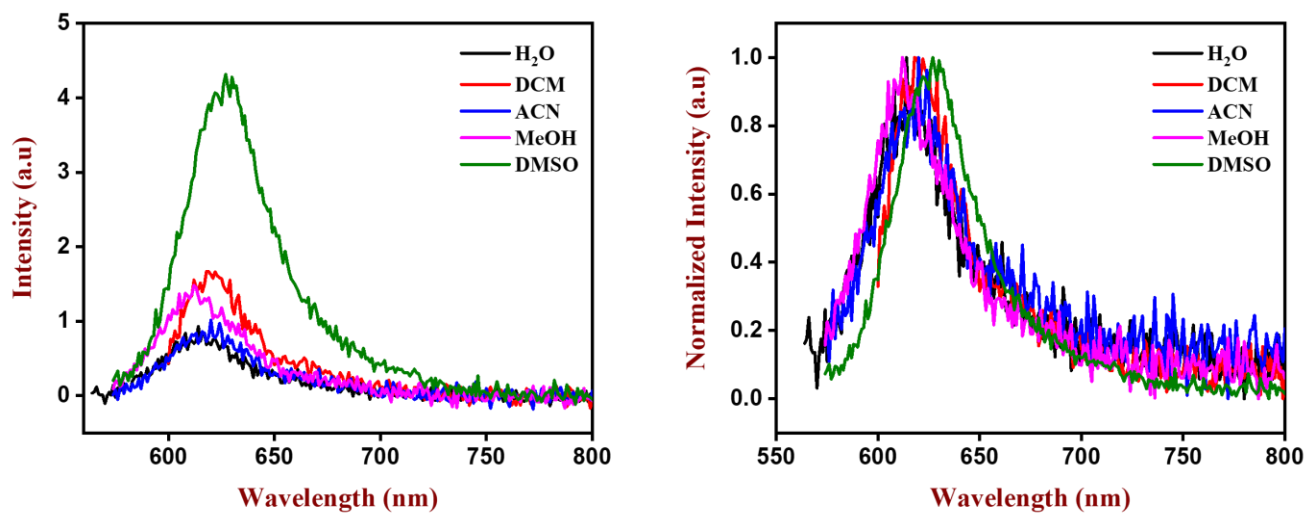


Figure S4: Emission spectra and normalized spectra of BTZ-JLD in different solvents

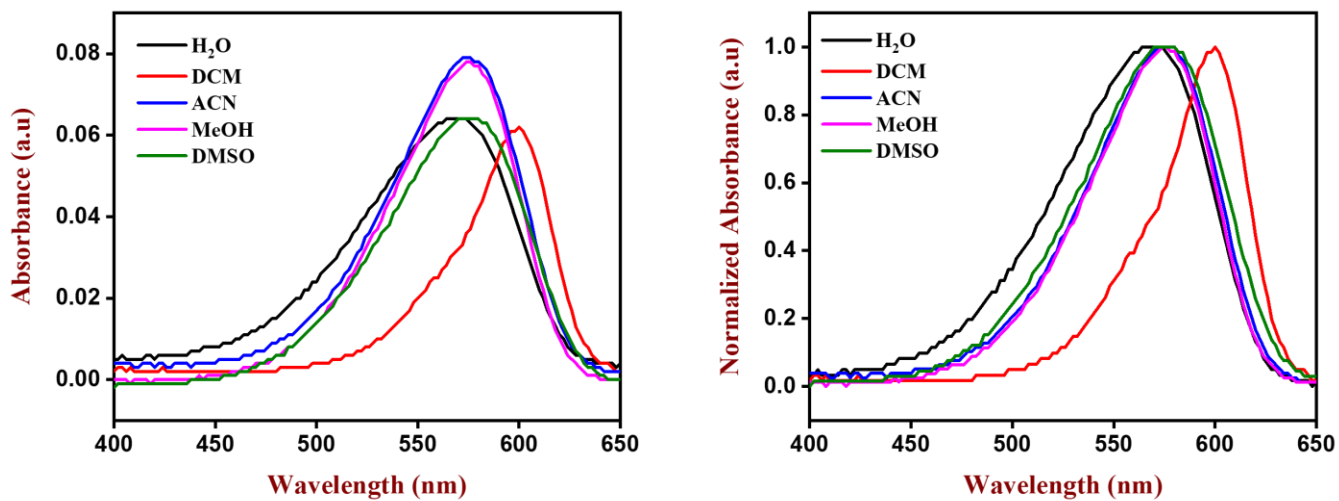


Figure S5: Absorption spectra and their normalized spectra of SEZ-JLD in different solvents

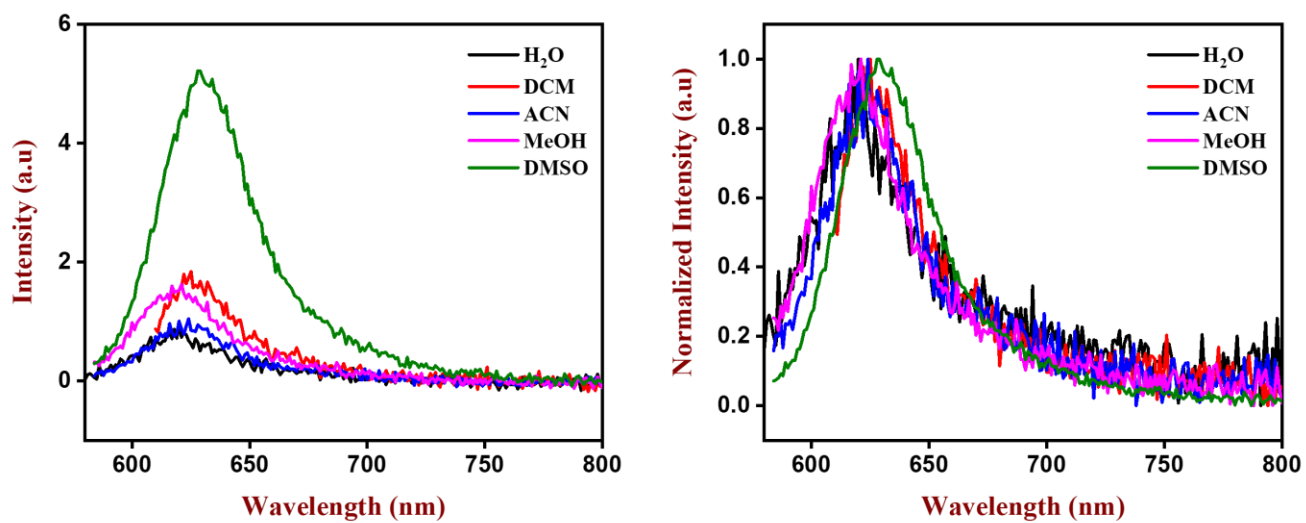


Figure S6: Emission spectra and normalized spectra of SEZ-JLD in different solvents

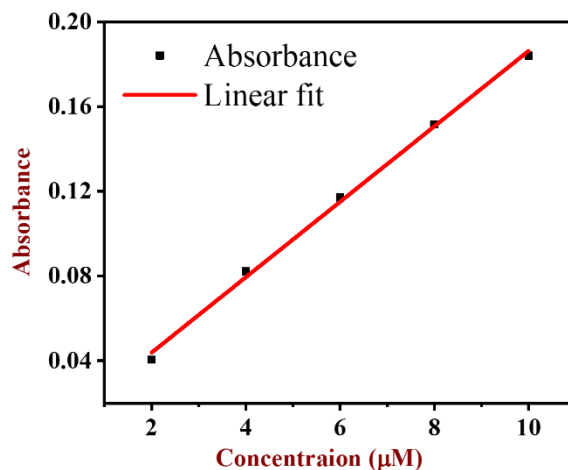
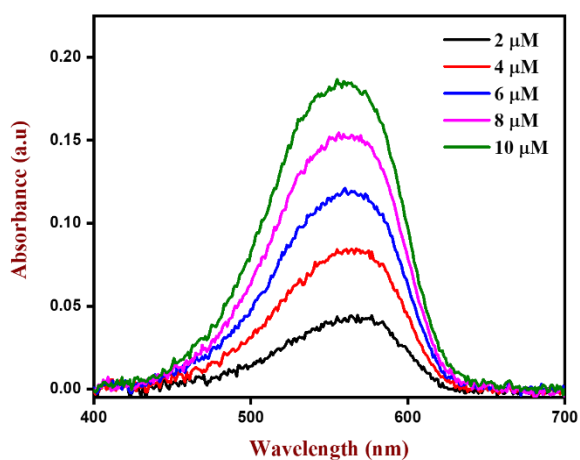


Figure S7: Absorption spectra of SEZ-JLD at different concentration in PBS. Linear fit of absorption vs concentration.

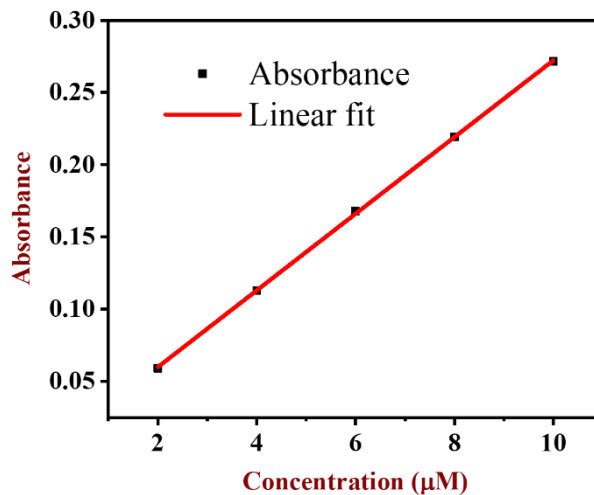
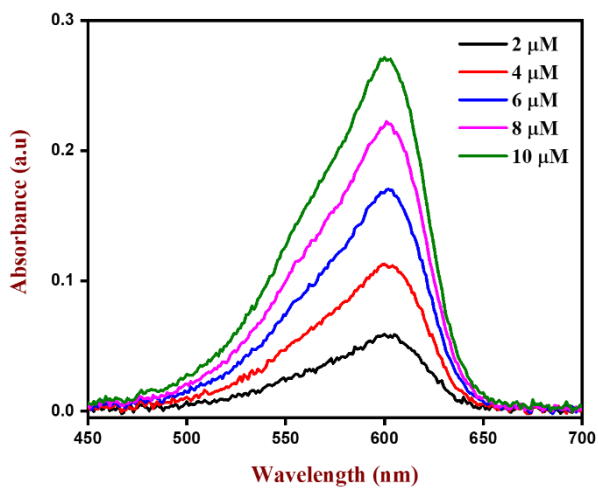


Figure S8: Absorption spectra of SEZ-JLD at different concentration in the presence of RNA. Linear fit of absorption vs concentration.

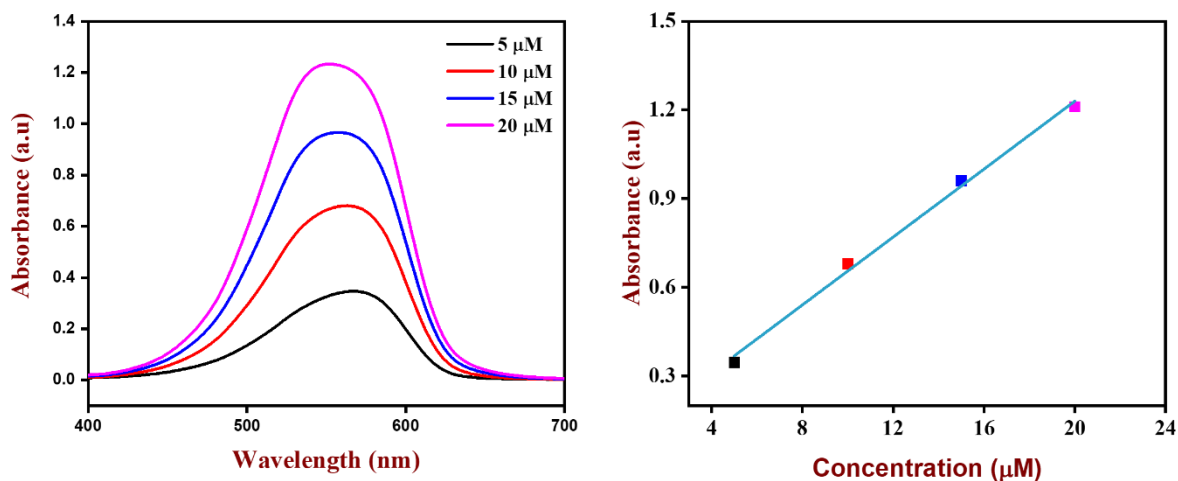


Figure S9: Absorption spectra of the probe SEZ-JLD at different concentrations in DMSO

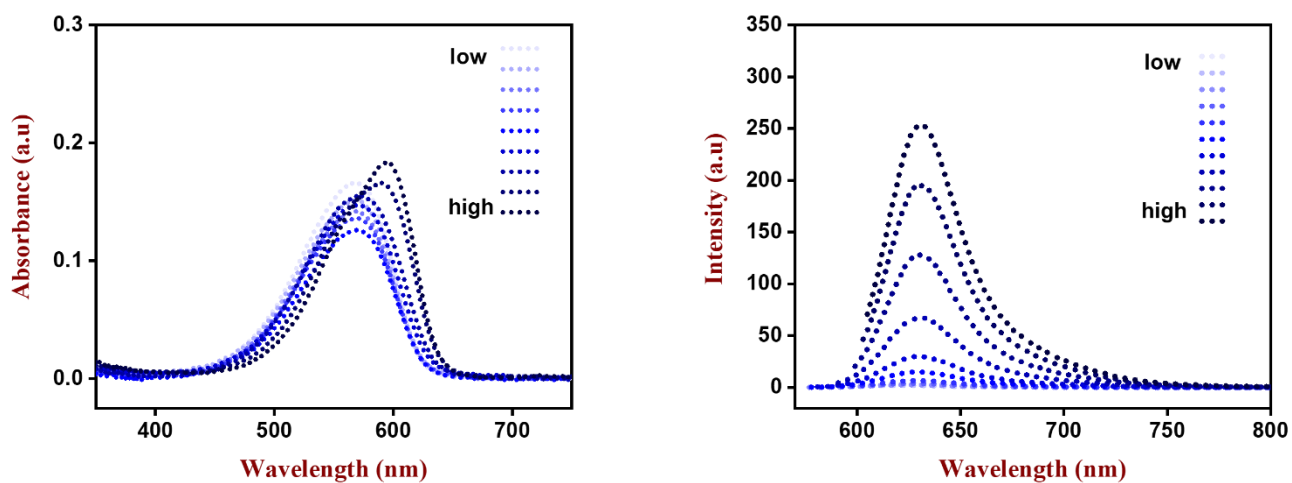


Figure S10: Optical response of SEZ-JLD with DNA at different concentration in PBS

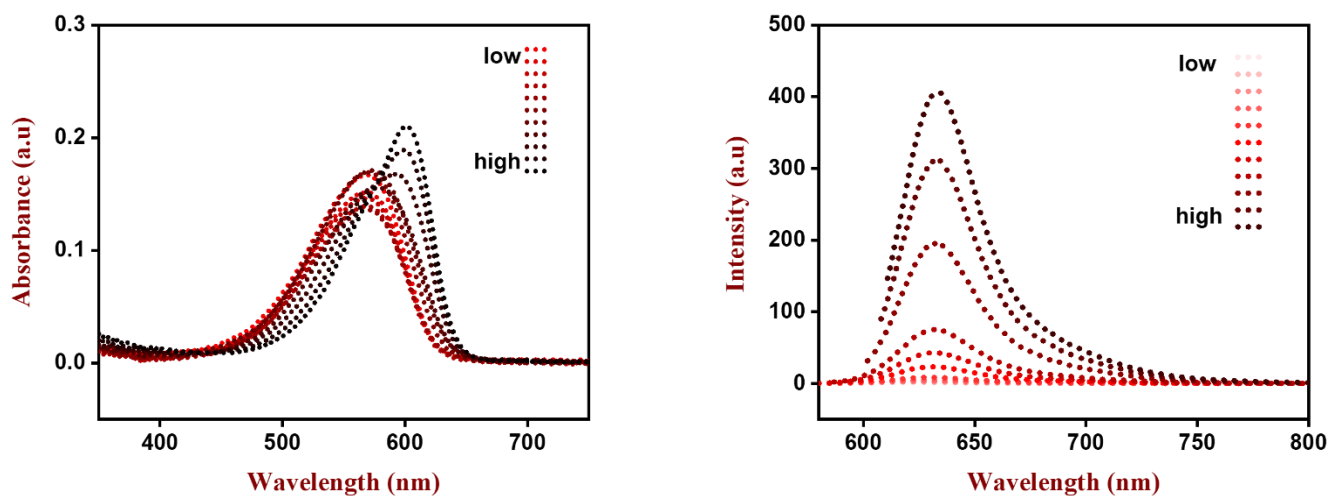


Figure S11: Optical response of SEZ-JLD with RNA at different concentration in PBS

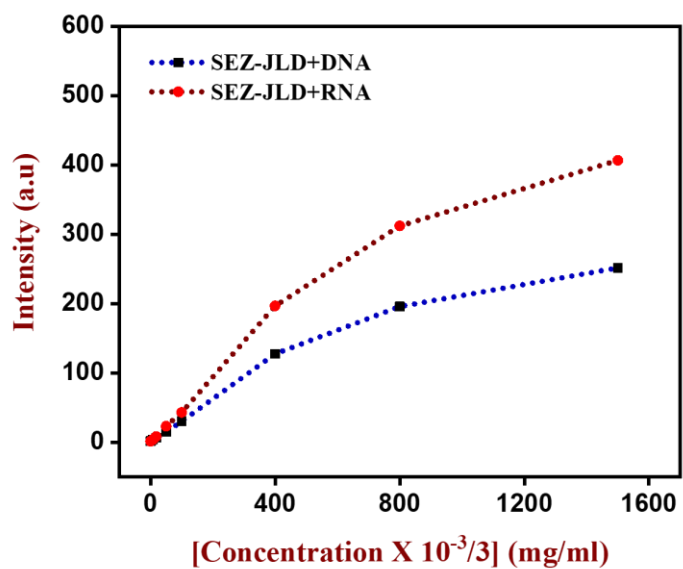


Figure S12: Fluorescence response of SEZ-JLD with DNA and RNA at different concentration

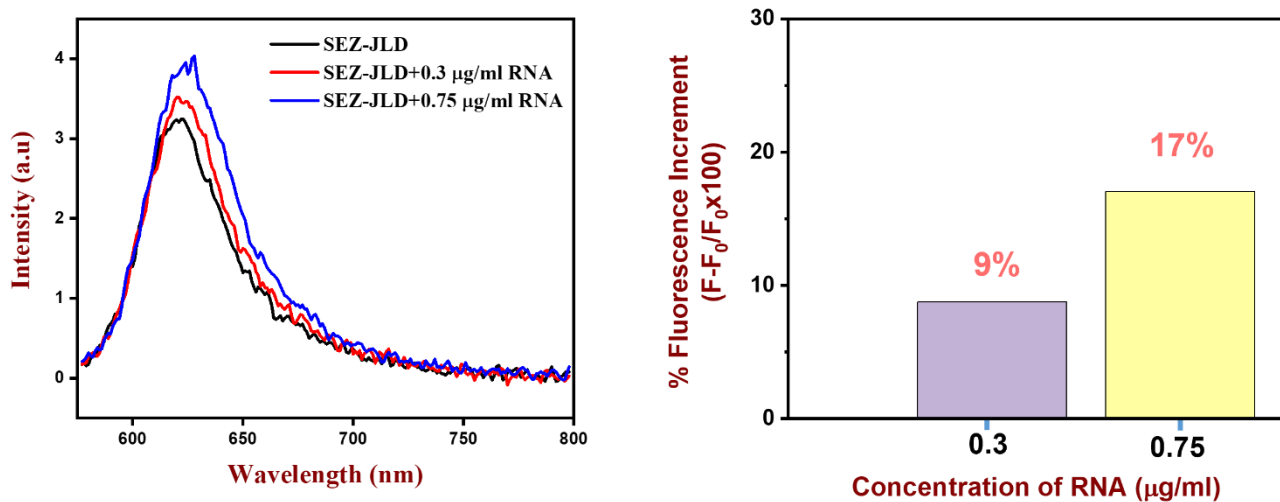


Figure S13: a) Detection limit of SEZ-JLD for RNA. b) Percentage of fluorescent increment in the presence of RNA

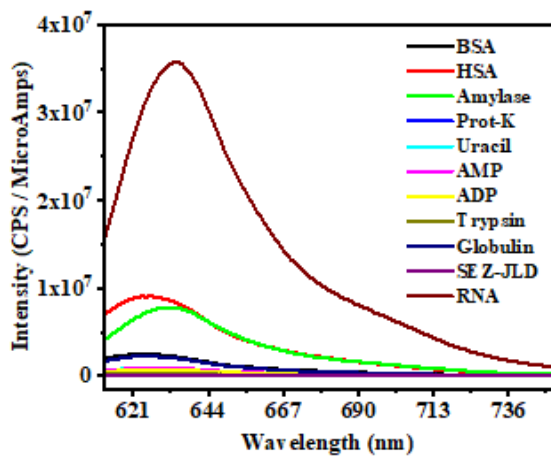


Figure S14: Selectivity of SEZ-JLD towards RNA (1mg/mL) over other biomolecules.

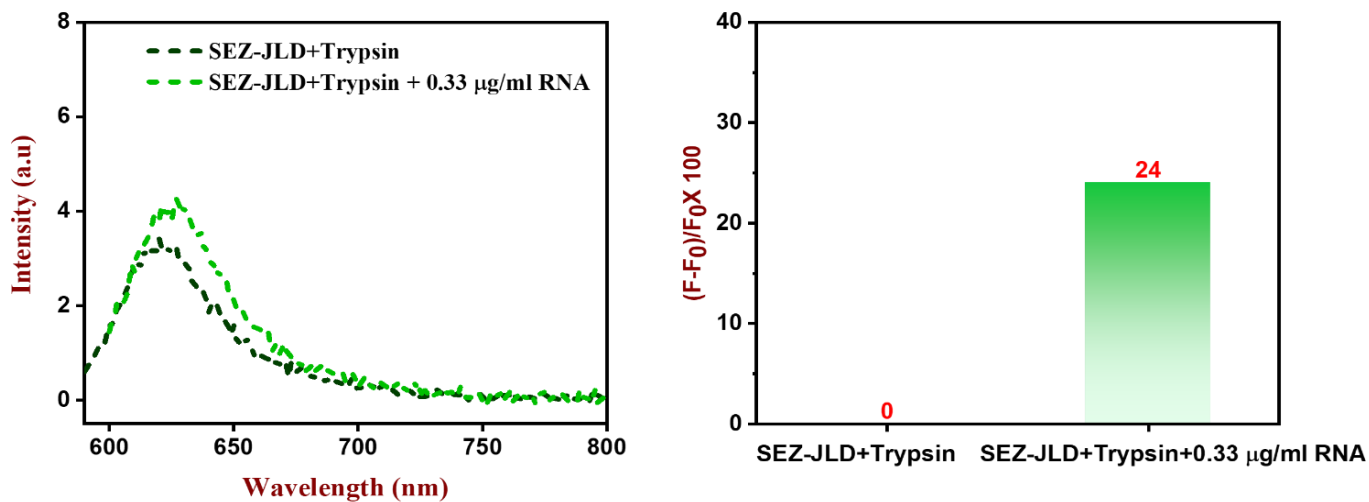


Figure S15: Sensitivity of SEZ-JLD towards RNA in the presence of trypsin (1 mg/ml).

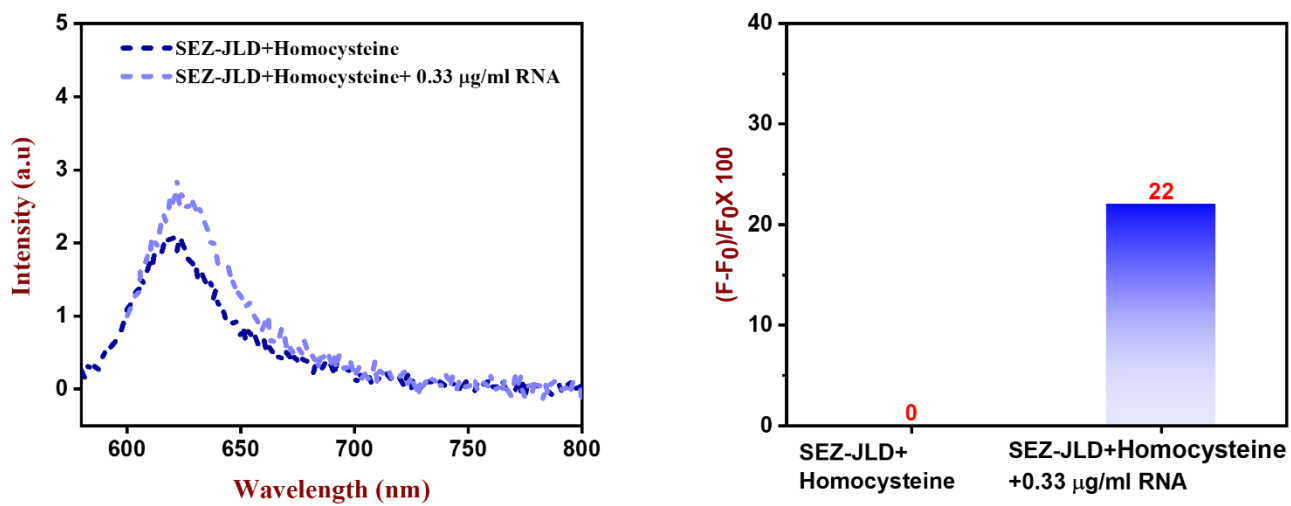


Figure S16: Sensitivity of SEZ-JLD towards RNA in the presence of homocysteine (1 mg/ml).

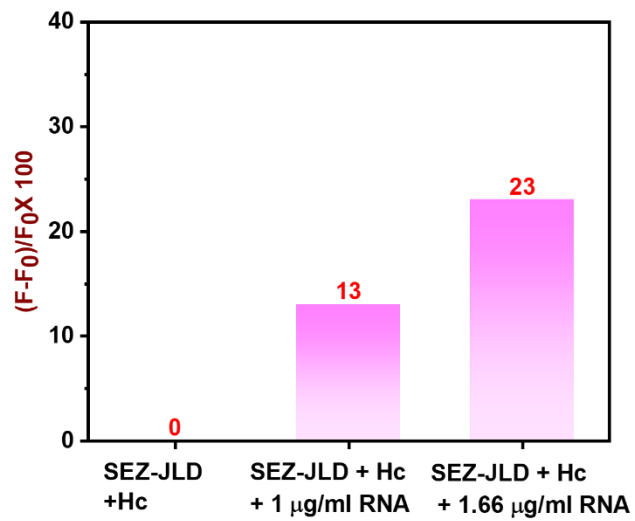
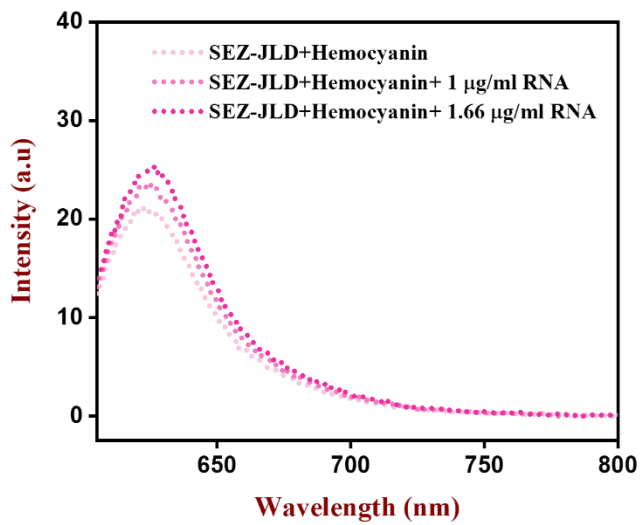


Figure S17: Sensitivity of SEZ-JLD towards RNA in the presence of hemocyanin (1mg/ml).

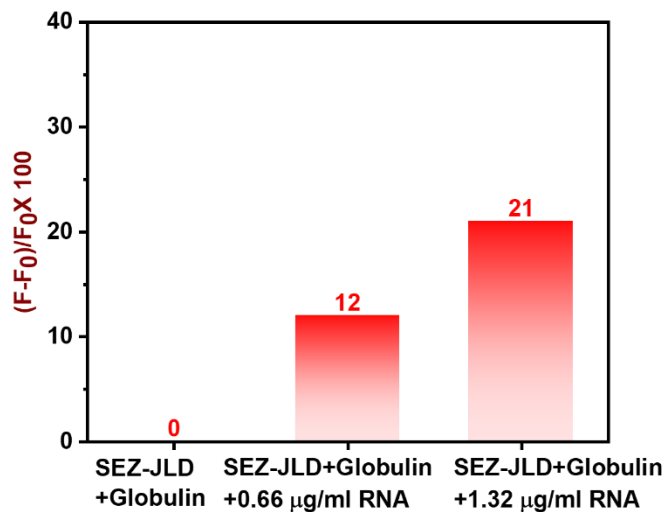
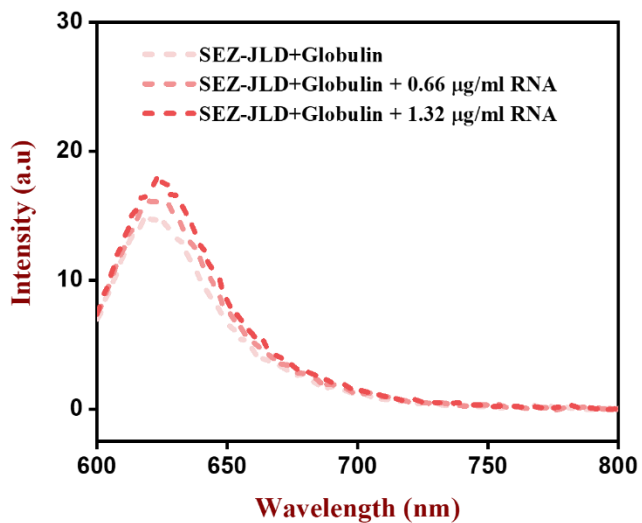


Figure S18: Sensitivity of SEZ-JLD towards RNA in the presence of globulin (1 mg/ml).

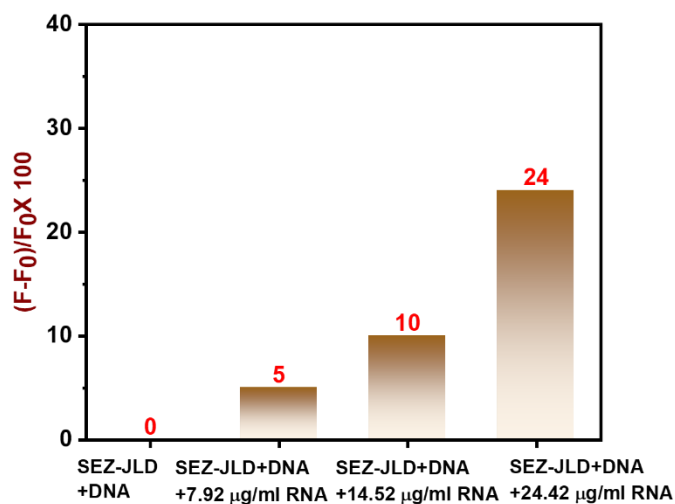
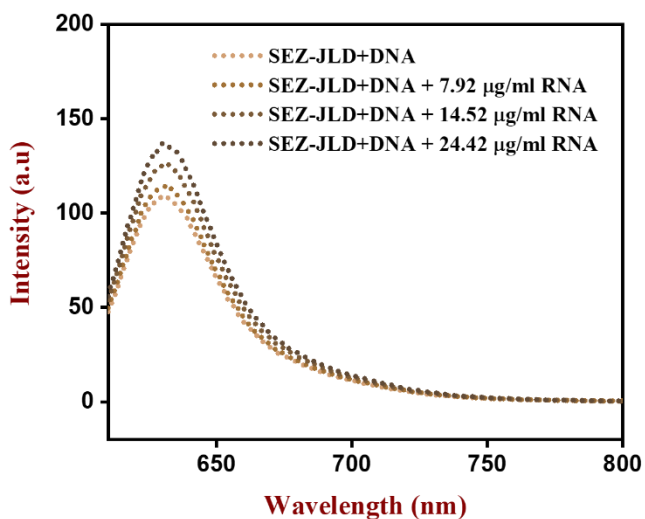


Figure S19: Sensitivity of SEZ-JLD towards RNA in the presence of DNA (1mg/ml).

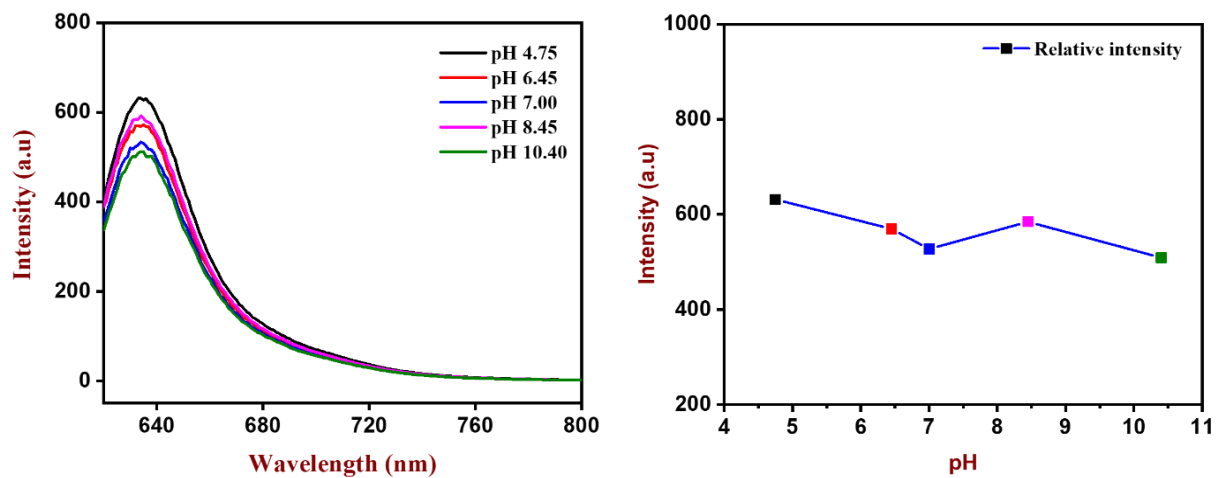


Figure S20: Effect of pH on fluorescence response of the probe (5 μ M) with RNA (1mg/mL) in PBS

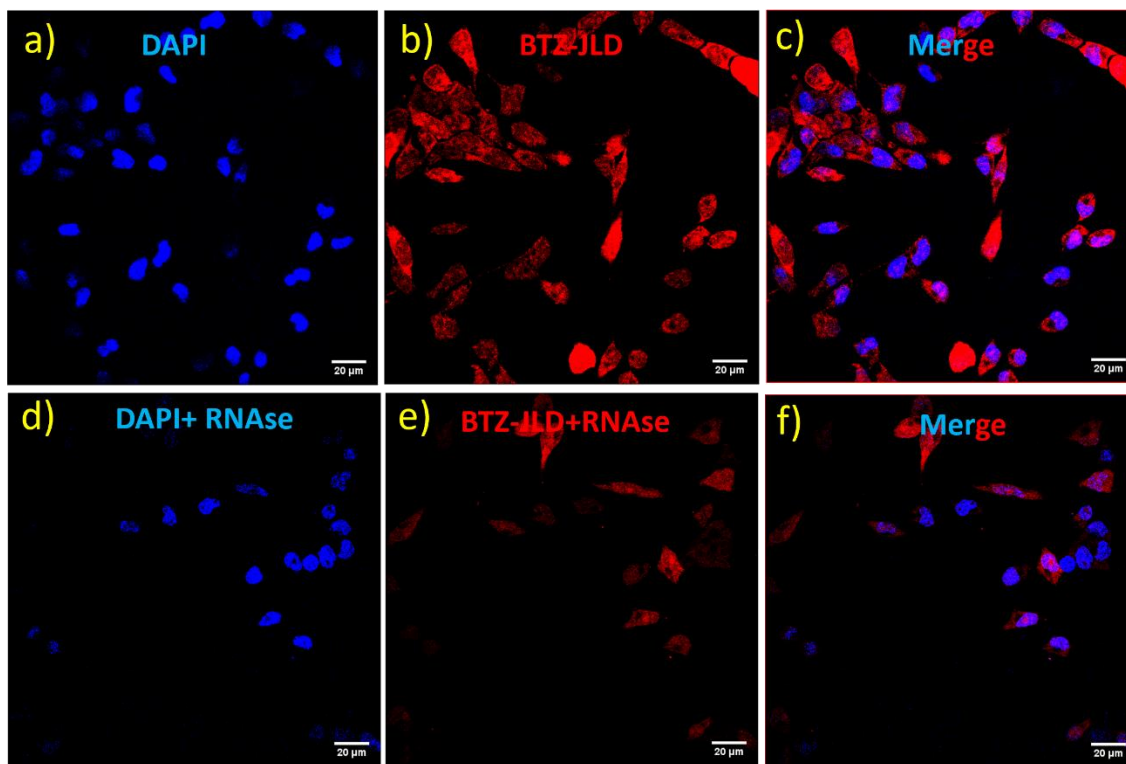


Figure S21 : Localization of the compounds in live HepG2 cells: a) DAPI, b) BTZ-JLD, c) overlay of a) and b) images. RNase digest test of the probe: i, j) RNase treated cells stained with DAPI and BTZ-JLD, respectively. k) Overlay of i) and j) images. The concentration of the probe was fixed to 5 μM for all imaging studies; $\lambda_{\text{ex}} = 561 \text{ nm}$ and emission filter 570-620 nm were set to visualize SEZ-JLD. $\lambda_{\text{ex}} = 405 \text{ nm}$ and emission filter 425-475 nm were set to visualize DAPI.

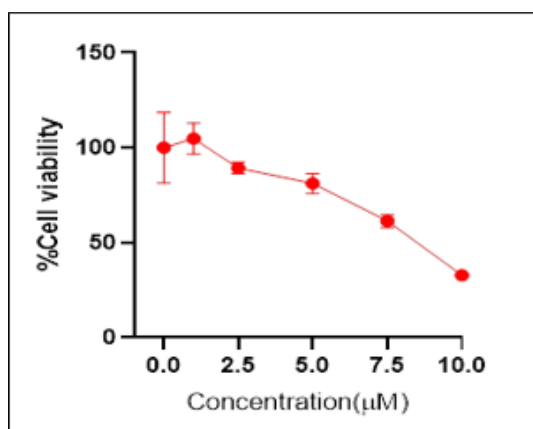


Figure S22: Cell viability test of the probe. Cell viability of HepG2 cells after 24 hours incubation of SEZ-JLD at different concentration. Viability of control cells (untreated HepG2 cells) was considered as 100% and the cell viability was evaluated relative to them. Results are mean \pm SD.

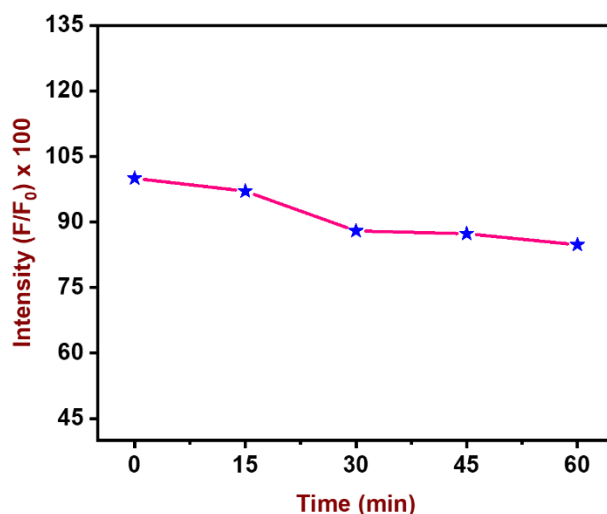


Figure S23: Intensity versus time plot showing the quantification of the photostability of the probe SEZ-JLD under continuous exposure of Mercury vapor lamp (160 W, 2.1×10^3 Lux).

Synthesis and Characterization:

Synthetic Procedure for A3:

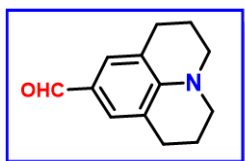
CuI (173 mg, 0.91 mmol, 0.2 equiv) and 1,10-phenanthroline (L) (164 mg, 0.91 mmol, 0.2 equiv) were added sequentially to 10 mL DMF under N₂ atmosphere and stirred for 20 min. To this orange-colored solution of CuI/L, succinimide (450 mg, 4.56 mmol, 1 equiv), 2-iodo aniline (**1**) (1.0 g, 4.56 mmol, 1 equiv), selenium powder (720 mg, 9.12 mmol, 2 equiv) and potassium carbonate (945 mg, 6.84 mmol, 1.5 equiv) were added in same order, and the resulted reaction mixture was stirred at 140 °C for 16 h. After this, the reaction mixture was poured into a beaker containing brine solution (80 mL) and the resulting solution was stirred for 2 h in air. The reaction mixture was extracted with ethyl acetate (25 mL x 3). The combined organic layer was washed with water (50 mL), dried over Na₂SO₄ and evaporated under vacuum. The crude product obtained after evaporating the ethyl acetate layer was purified by column chromatography on silica gel using hexane and ethyl acetate as mobile phase (8:2) which resulted in the isolation of bis(2-aminophenyl) diselenide (**2**). This was converted into a crystalline orange solid on standing. It was used in the next step without characterization.³

In a round bottom flask, bis(2-amino phenyl) diselenide (**2**) (0.3 mmol) was taken in glycerol (5 mL). Then 50 wt% (in water) phosphinic acid (100 μL) was added into the reaction mixture under the nitrogen atmosphere and left for stirring for 30 minutes at 90 °C. Then acetylacetone (0.5 mmol) was added to the reaction mixture and heated for an additional 1 hour at 90 °C. After completion of the reaction, the reaction mixture in water was extracted with EtOAc. The organic portion was dried over sodium sulphate and concentrated under a vacuum to obtain light yellow liquid 2-methyl benzoselenazole (**3**).⁴ It was further stirred with methyl iodide in acetonitrile to get respective 2,3-dimethylbenzo[d][1,3]selenazol-3-ium salt (**A3**). The NMR and mass spectra of **A3** have been reported in our previous report.⁵

Similarly, cationic salts **A1** and **A2** were synthesized following literature-reported procedures.⁵

Synthetic Procedure for JLD-AI:

Phosphorous oxychloride (0.78 g, 5.0 mmol) was added dropwise to anhydrous DMF (1.11 g, 15.2 mmol) under nitrogen with ice-bath cooling. After addition, the mixture was stirred at room temperature for 30 min, transferred to a flask containing julolidine (0.796 g, 4.6 mmol) and the resulting mixture was heated to 90 °C for 4 h. After cooling, water (100 ml) was added to the reaction mixture and the mixture was neutralized with sodium bicarbonate. The mixture was then extracted with ethyl acetate, washed with brine, and dried over magnesium sulfate. The solvent was removed under vacuum and the residue was purified by flash chromatography (hexane/ethyl acetate, 4:1) to give the product a light-yellow solid.



1,2,3,5,6,7-Hexahydroprido[3,2,1-ij] quinoline-9-carbaldehyde (JLD-AI): Light yellow solid, Yield: 85%. ^1H NMR (500 MHz, CDCl_3): δ = 9.59 (s, 1H), 7.29 (s, 2H), 3.30-3.28 (m, 4H), 2.78-2.75 (m, 4H), 1.98-1.93 (m, 4H) ppm. ^{13}C NMR (125 MHz, CDCl_3): 190.27, 147.98, 129.59, 124.04, 120.39, 50.11, 27.73, 21.32 ppm. MS: m/z calculated for $\text{C}_{13}\text{H}_{15}\text{NNaO}$ $[\text{M}+\text{Na}]^+$ 224.1048, found 224.1049, Mass Error: 0.45 ppm.

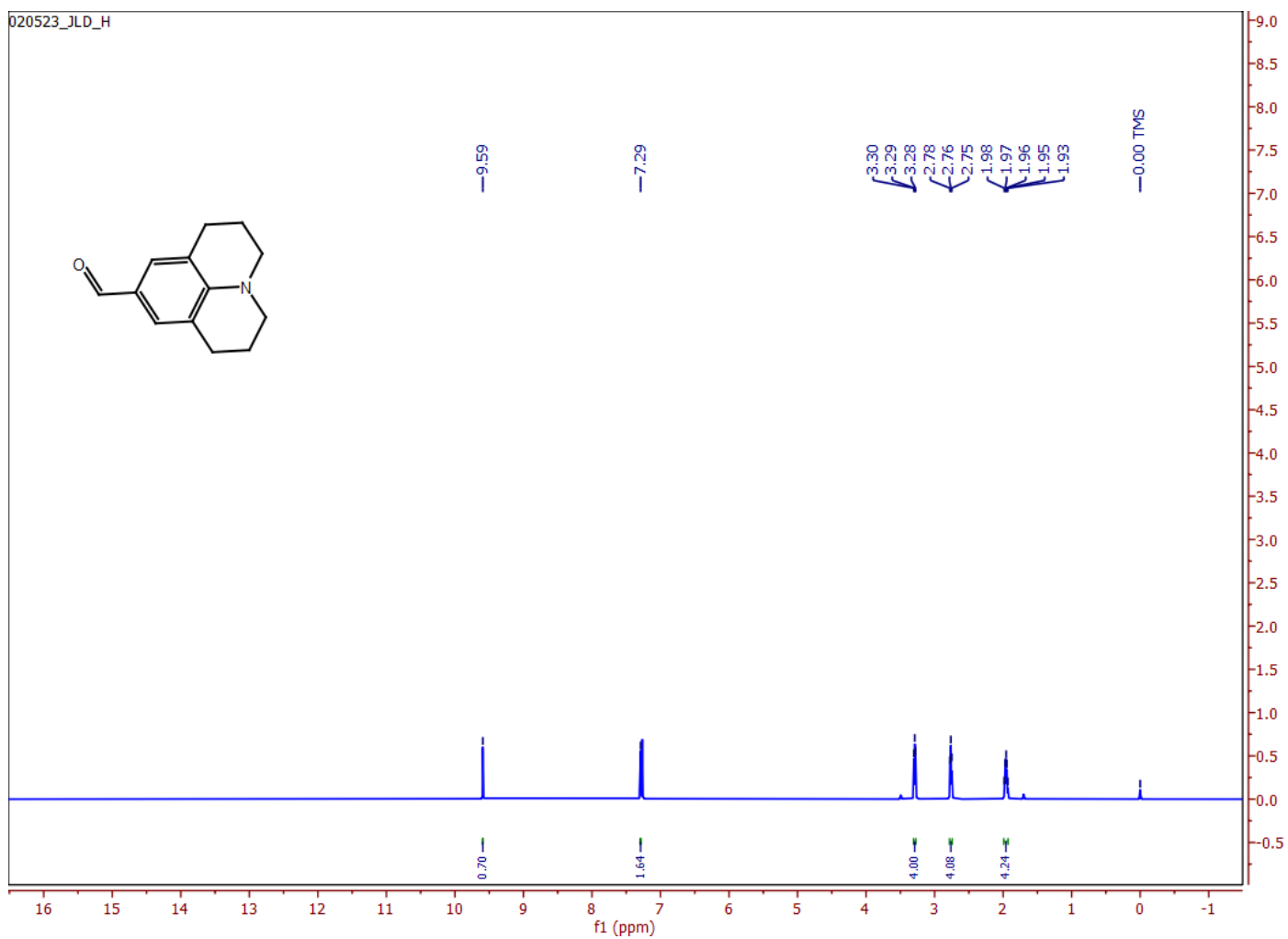


Figure S24: ^1H NMR of JLD-AI in CDCl_3 .

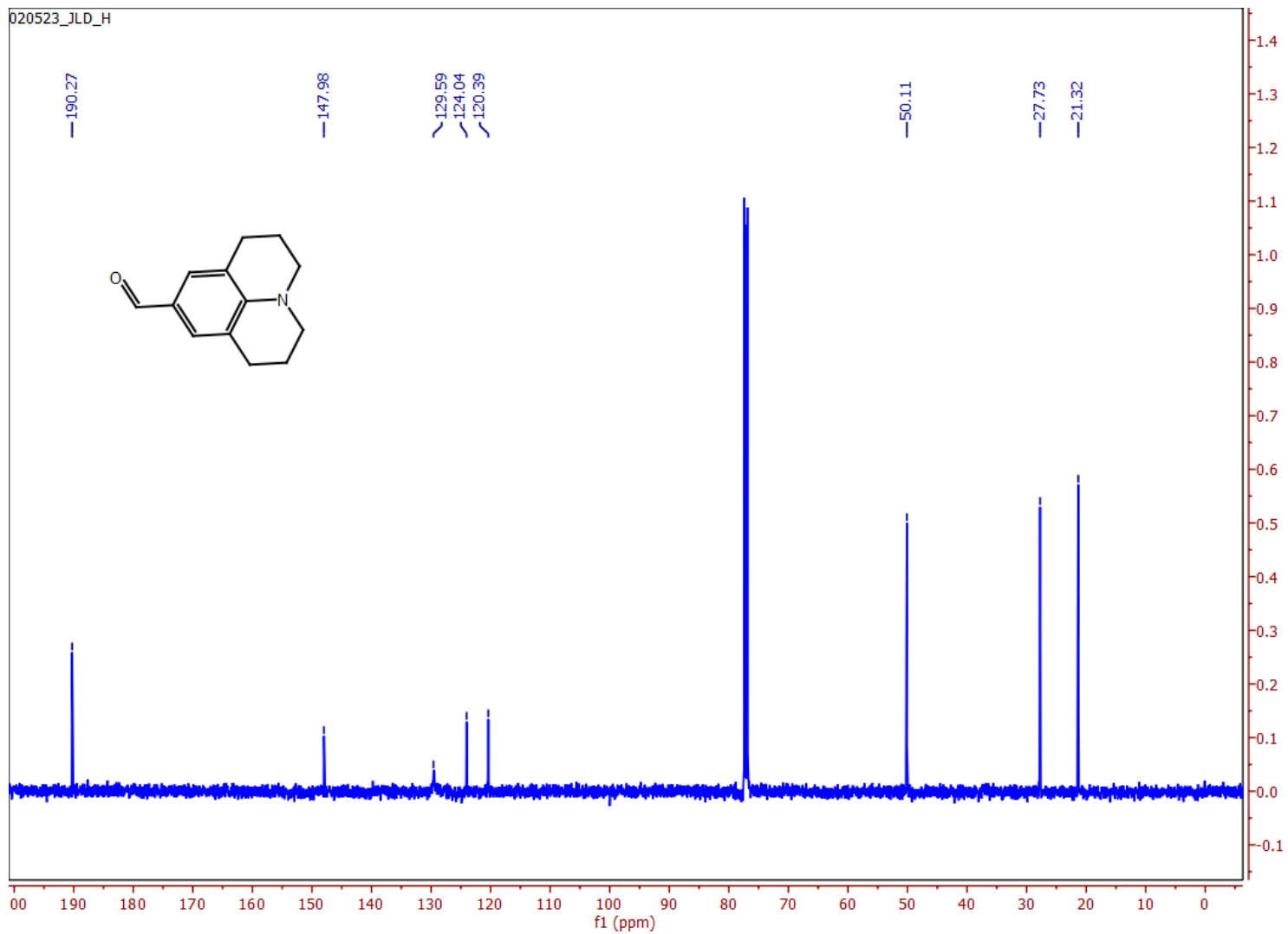


Figure S25: ^{13}C NMR of JLD-AI in CDCl_3 .

Analysis Name D:\Data\User Data\swar\JLD-AL.d
Method Tune_pos_Standard.m
Sample Name
Comment

Operator HRMS
Instrument maXis impact 1819696.00160

Acquisition Parameter

Source Type	ESI	Ion Polarity	Positive	Set Nebulizer	0.5 Bar
Focus	Active	Set Capillary	4500 V	Set Dry Heater	200 °C
Scan Begin	50 m/z	Set End Plate Offset	-500 V	Set Dry Gas	4.0 l/min
Scan End	1500 m/z	Set Charging Voltage	2000 V	Set Divert Valve	Source
		Set Corona	0 nA	Set APCI Heater	0 °C

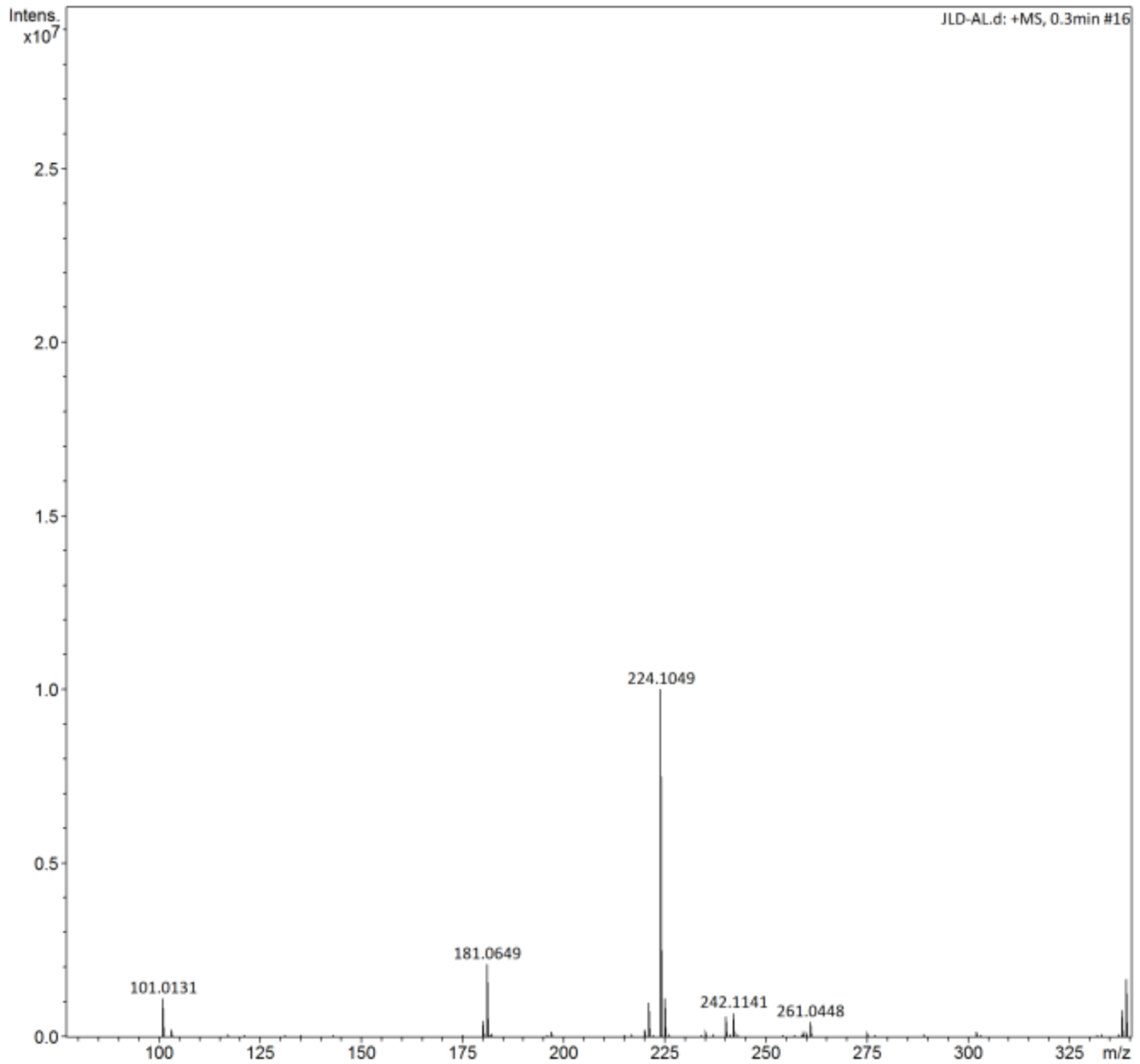


Figure S26: MS of JLD-AI

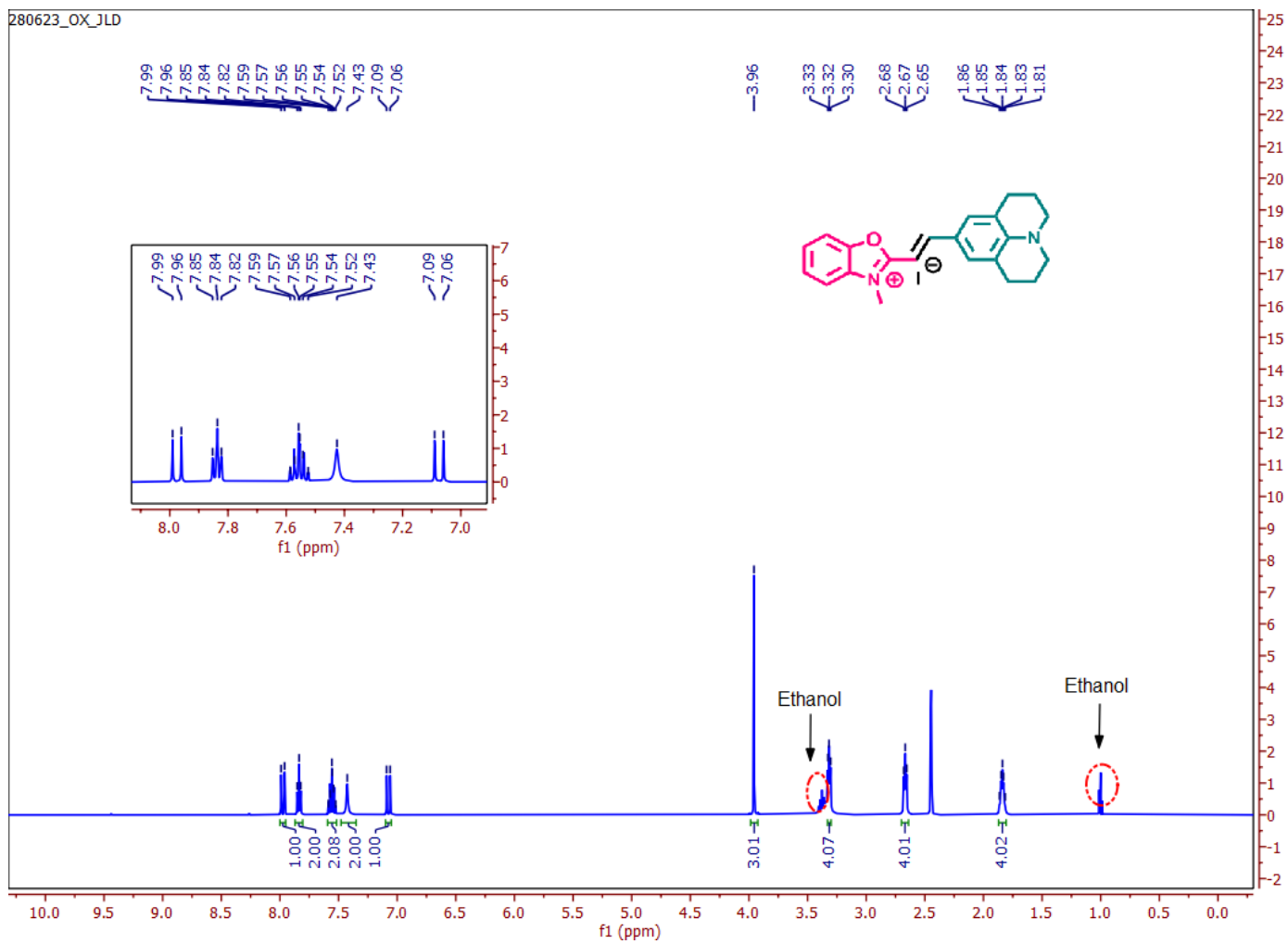


Figure S27: ^1H NMR of OX-JLD in $\text{DMSO-}d_6$.

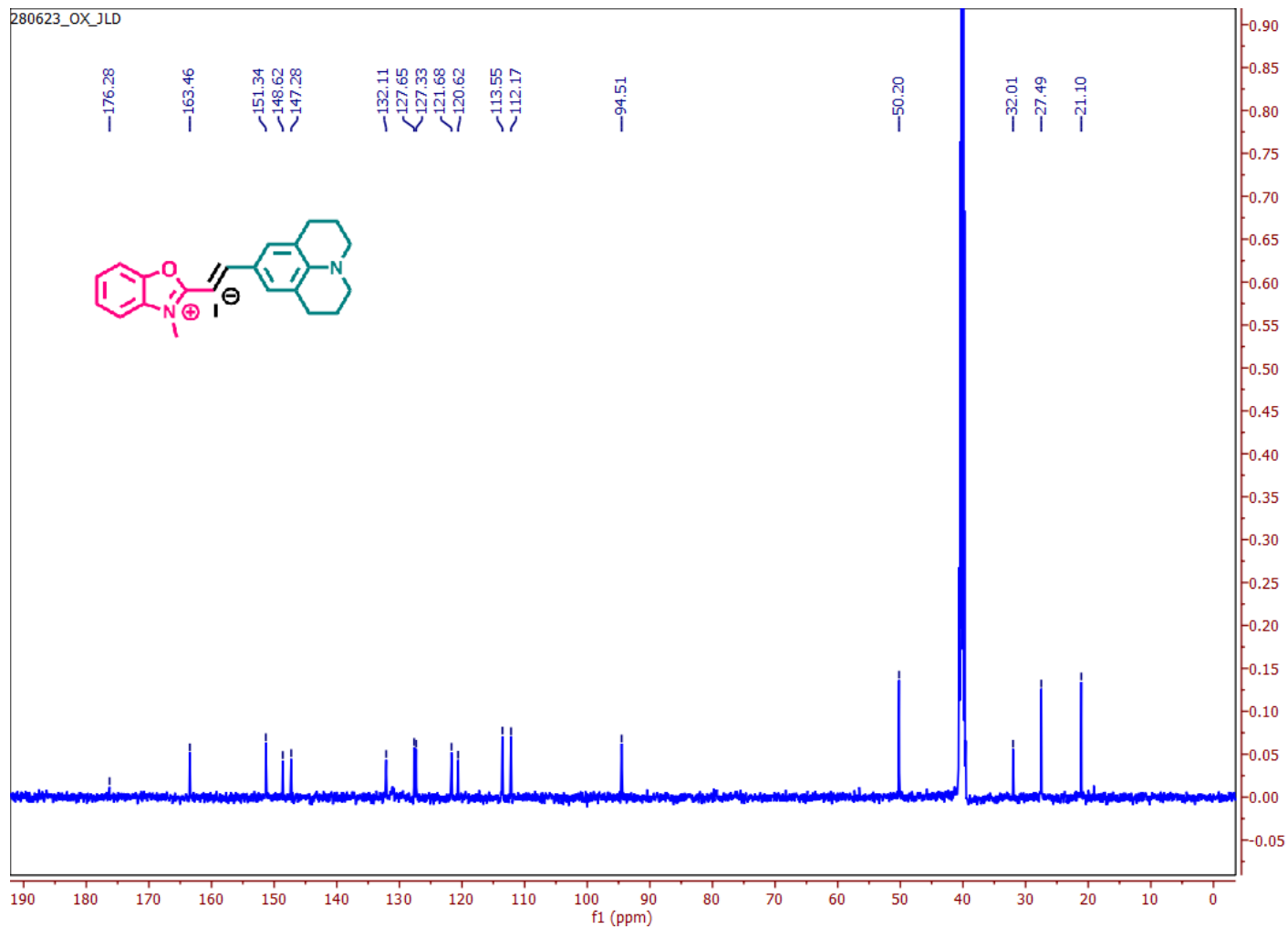


Figure S28: ^{13}C NMR of OX-JLD in $\text{DMSO-}d_6$

Display Report

Analysis Info

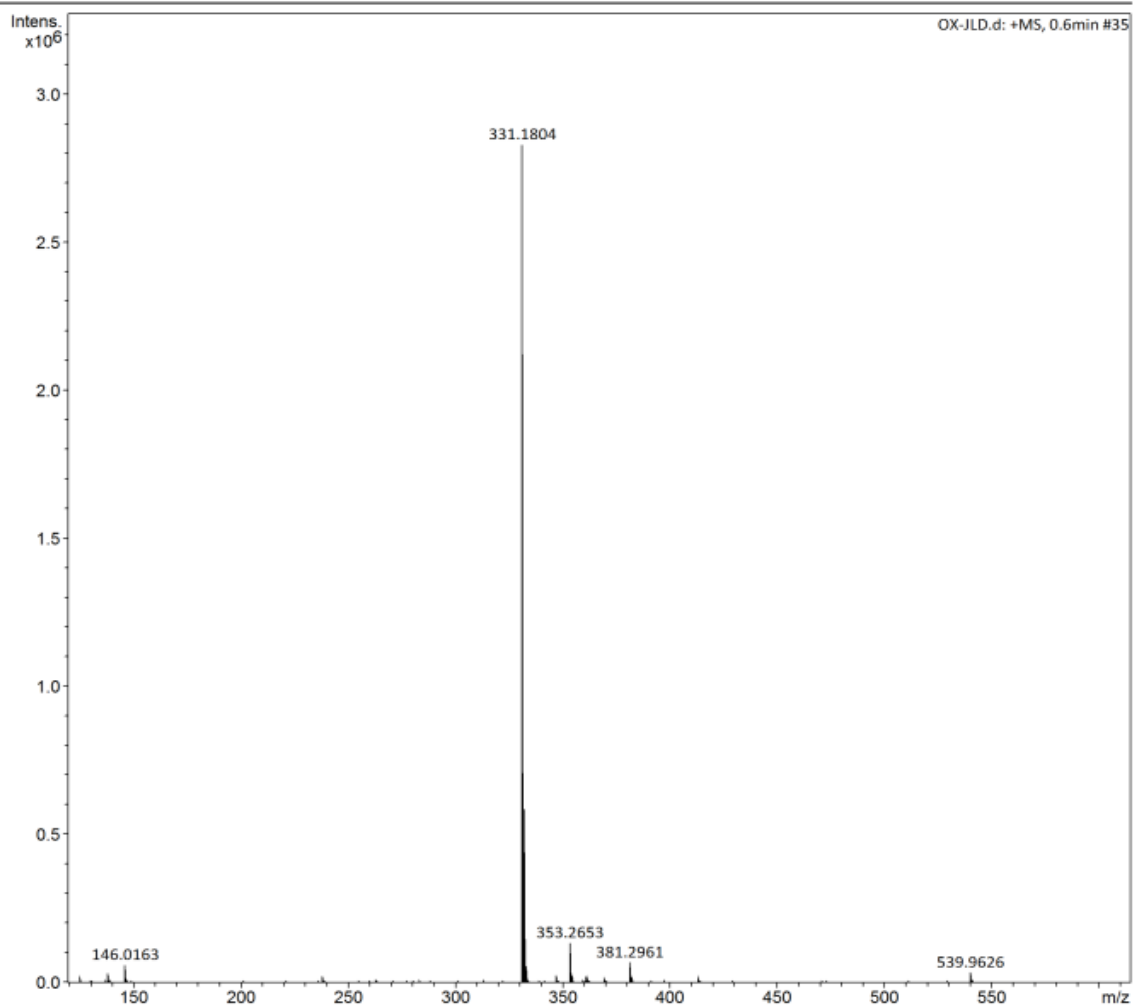
Analysis Name D:\Data\User Data\lswar\OX-JLD.d
Method Tune_pos_Standard.m
Sample Name
Comment

Acquisition Date 6/23/2023 12:56:21 PM

Operator HRMS
Instrument maXis impact 1819696.00160

Acquisition Parameter

Source Type	ESI	Ion Polarity	Positive	Set Nebulizer	0.5 Bar
Focus	Active	Set Capillary	4500 V	Set Dry Heater	200 °C
Scan Begin	50 m/z	Set End Plate Offset	-500 V	Set Dry Gas	4.0 l/min
Scan End	1500 m/z	Set Charging Voltage	2000 V	Set Divert Valve	Source
		Set Corona	0 nA	Set APCI Heater	0 °C



OX-JLD.d

Bruker Compass DataAnalysis 4.1

printed: 6/23/2023 12:58:14 PM

by: HRMS

Page 1 of 1

Figure S29: MS of OX-JLD

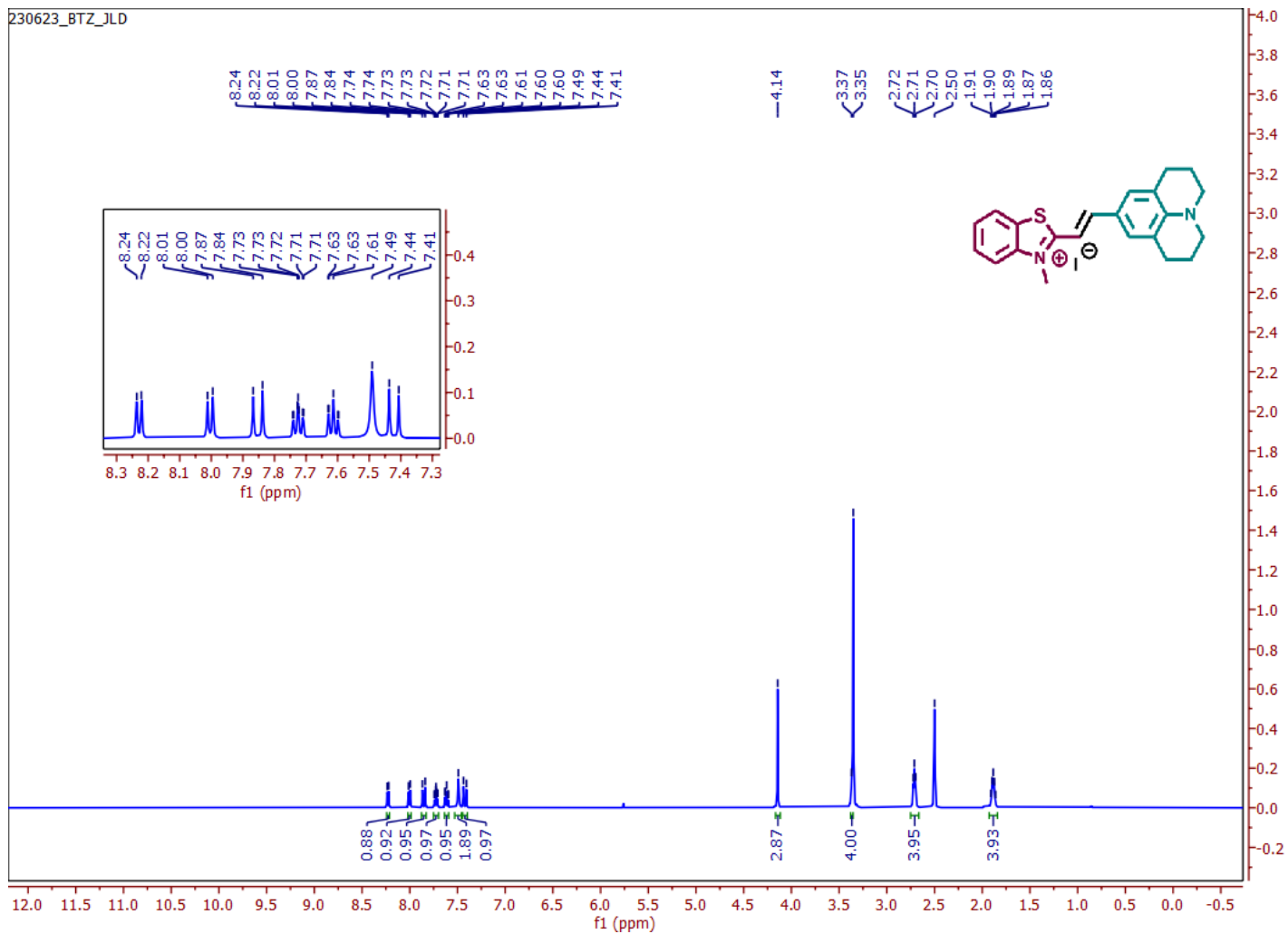


Figure S30: ^1H NMR of BTZ-JLD in $\text{DMSO-}d_6$.

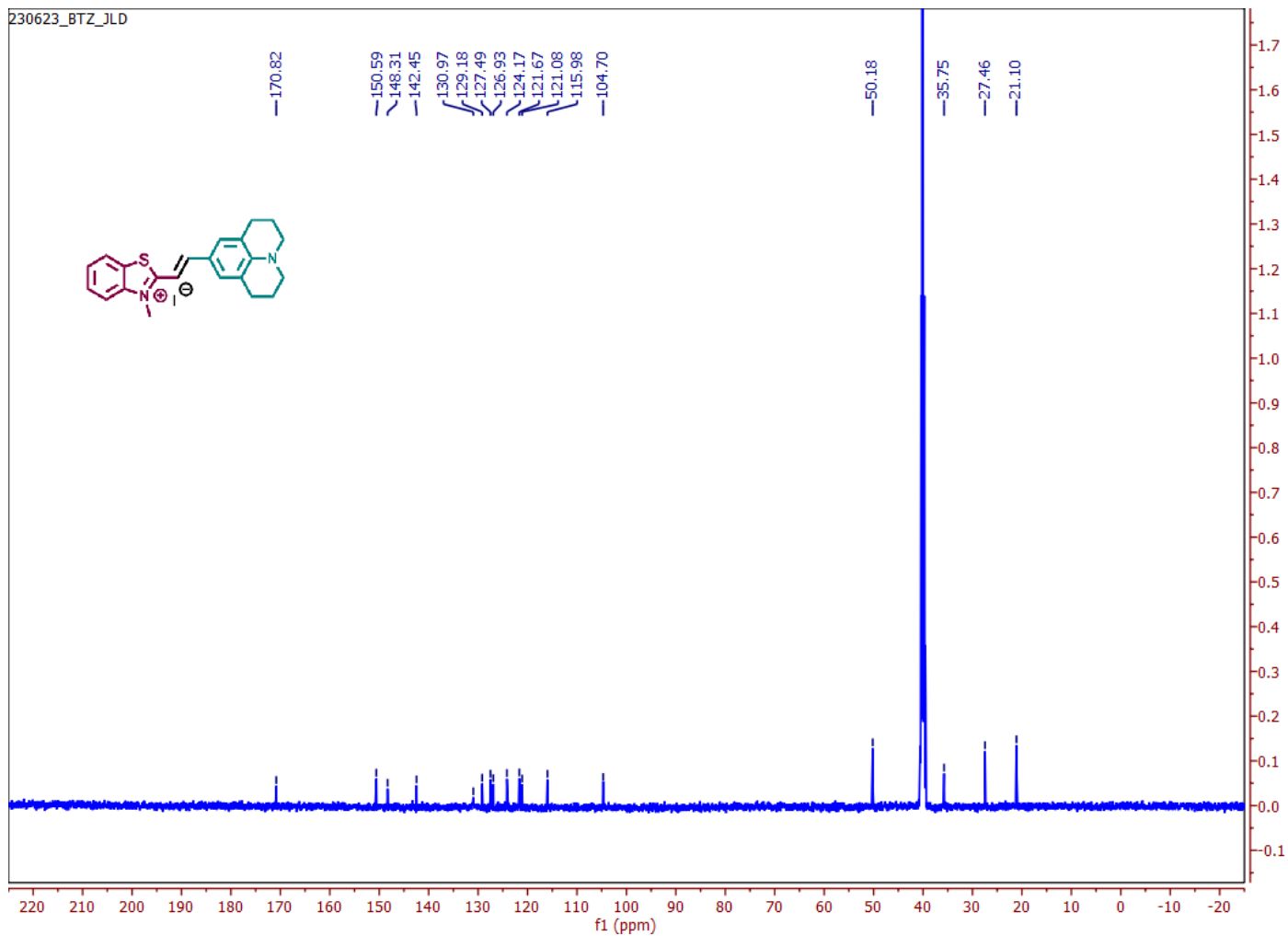


Figure S31: ^{13}C NMR of BTZ-JLD in $\text{DMSO-}d_6$

Display Report

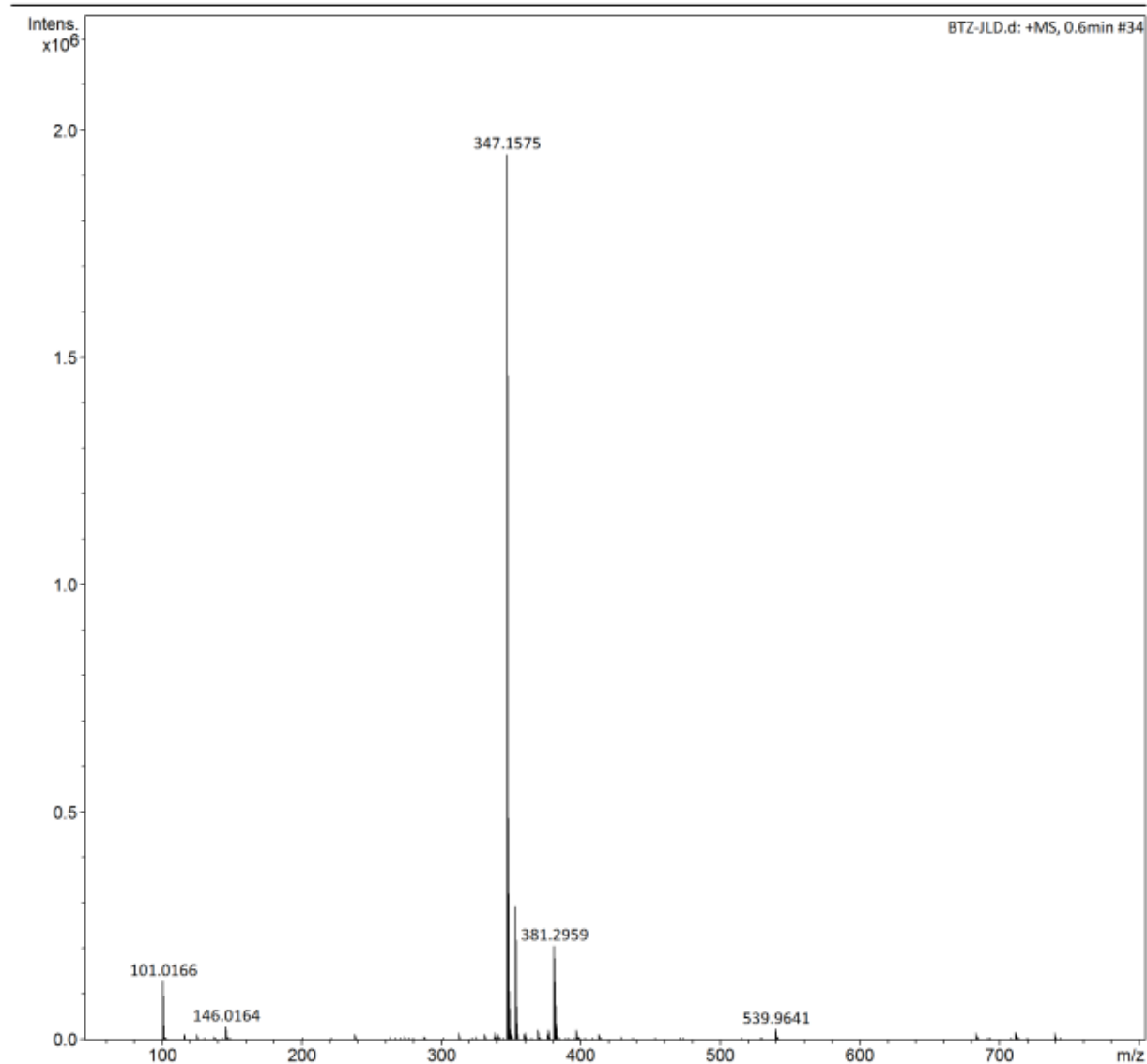
Analysis Info

Analysis Name D:\Data\User Data\swar\BTZ-JLD.d
Method Tune_pos_Standard.m
Sample Name
Comment

Acquisition Date 6/23/2023 12:49:14 PM
Operator HRMS
Instrument maXis impact 1819696.00160

Acquisition Parameter

Source Type	ESI	Ion Polarity	Positive	Set Nebulizer	0.5 Bar
Focus	Active	Set Capillary	4500 V	Set Dry Heater	200 °C
Scan Begin	50 m/z	Set End Plate Offset	-500 V	Set Dry Gas	4.0 l/min
Scan End	1500 m/z	Set Charging Voltage	2000 V	Set Divert Valve	Source
		Set Corona	0 nA	Set APCI Heater	0 °C



BTZ-JLD.d

Bruker Compass DataAnalysis 4.1

printed: 6/23/2023 12:51:55 PM

by: HRMS

Page 1 of 1

Figure S32: MS of BTZ-JLD.

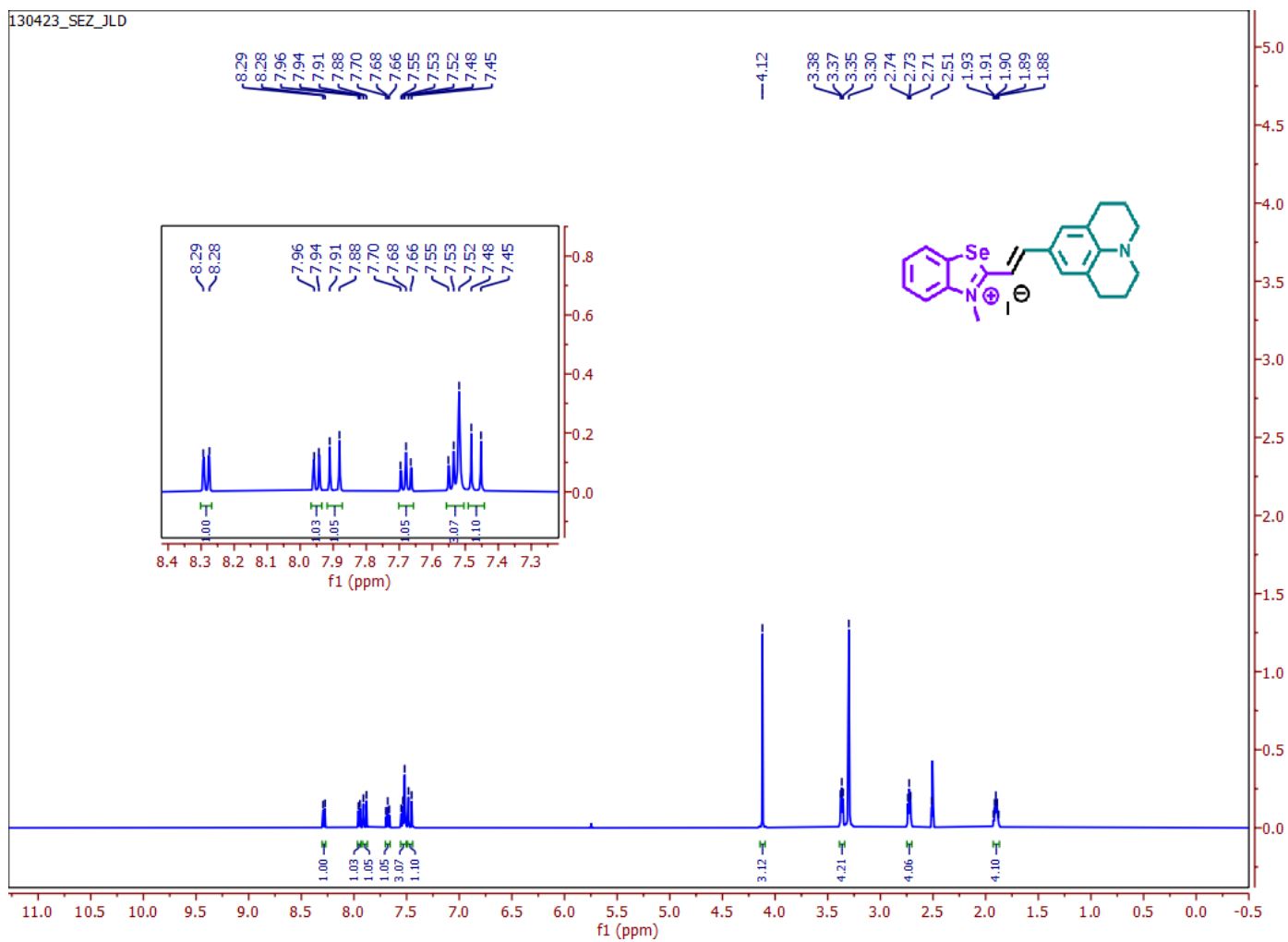


Figure S 33: ^1H NMR of SEZ-JLD in DMSO-d_6 .

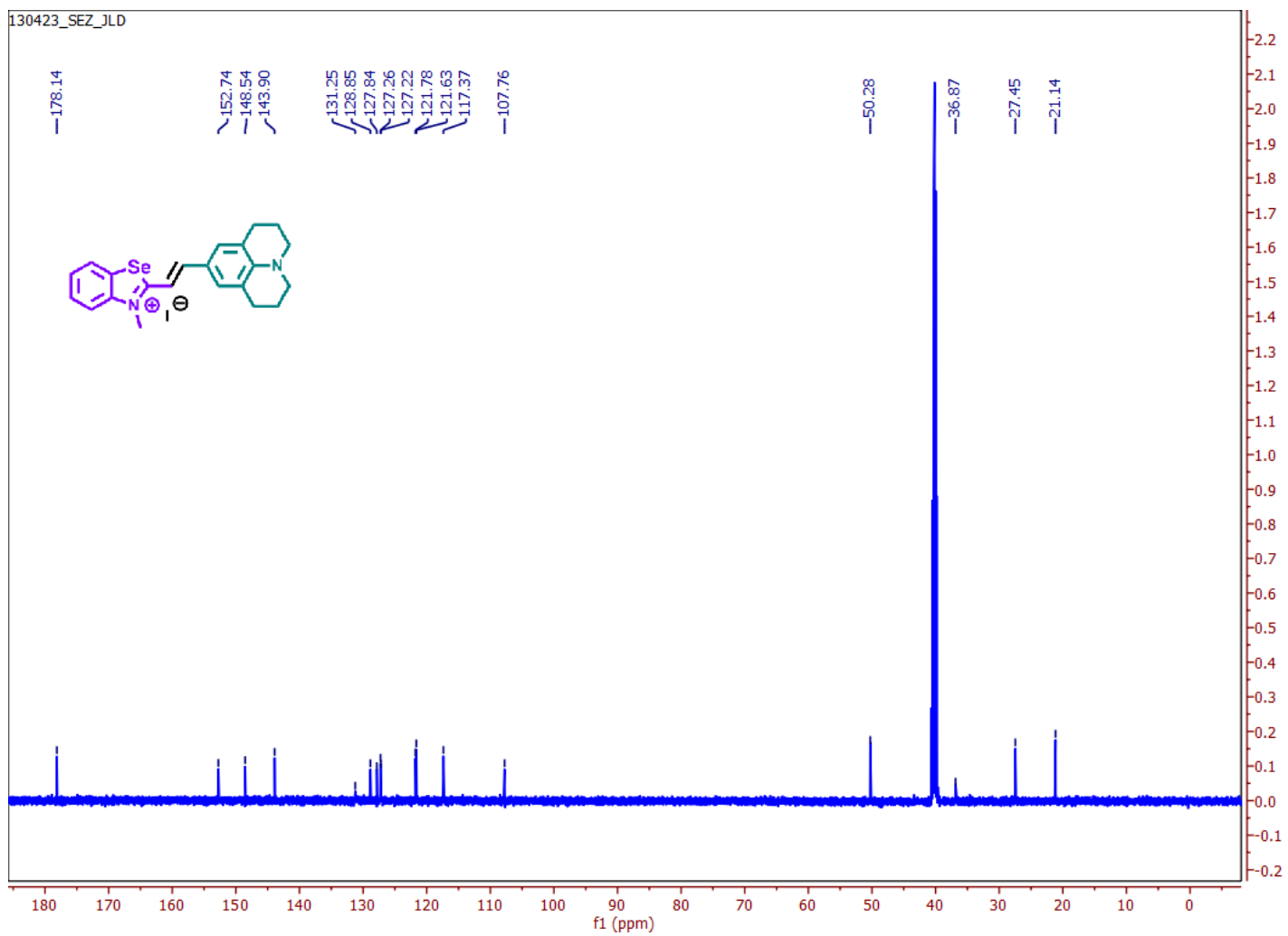


Figure S34: ^{13}C NMR of SEZ-JLD in DMSO-d_6 .

Single Mass Analysis

Tolerance = 20.0 PPM / DBE: min = -1.5, max = 50.0

Element prediction: Off

Number of isotope peaks used for i-FIT = 3

Monoisotopic Mass, Even Electron Ions

27 formula(e) evaluated with 1 results within limits (up to 50 closest results for each mass)

Elements Used:

C: 0-22 H: 0-50 N: 0-2 Se: 1-3

270423_26_03_SEZ_JLD 30 (0.320)

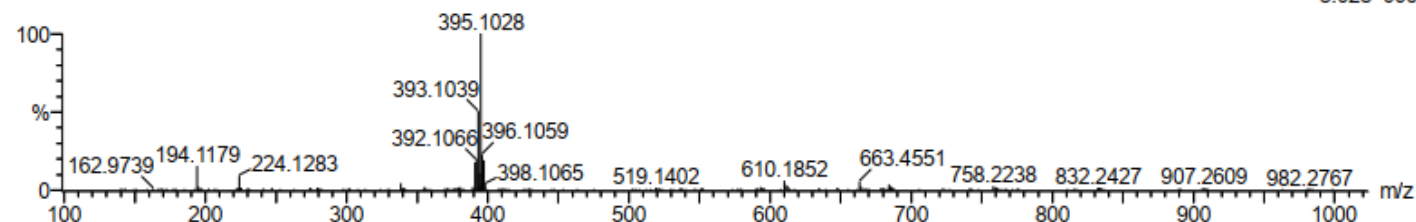
IITRPR

XEVO G2-XS QTOF
270423_26_03_SEZ_JLD

Test Name :

1: TOF MS ES+

3.02e+006



Minimum: -1.5
Maximum: 5.0 20.0 50.0

Mass	Calc. Mass	mDa	PPM	DBE	i-FIT	Norm	Conf (%)	Formula
395.1028	395.1026	0.2	0.5	13.5	967.1	n/a	n/a	C22 H23 N2 Se

Figure S35: MS of SEZ-JLD.

X-ray analysis:

Single-crystal X-ray diffraction data of compound **SEZ-JLD** were collected on an Agilent Supernova X-ray diffractometer fitted with a CCD detector at 150 K, using the graphite-monochromatic Cu K α radiation ($\lambda = 1.54184 \text{ \AA}$) source. To analyze the single crystal structure of SEZ-JLD, similar software and methods have been followed as reported earlier.⁶⁻¹⁰ For all the non-hydrogen atoms Least square refinements with anisotropic thermal motion parameters and isotropic ones for the hydrogen atoms were used. Crystallographic data is presented in Table S6. CCDC **2261160** contains the supplementary crystallographic data for this paper. These data can be obtained free of charge from The Cambridge Crystallographic Data Centre *via* www.ccdc.cam.ac.uk/data_request/cif.

Table S6. Crystal data and structure refinement for SEZ-JLD

Identification code	SEZ-JLD
Empirical formula	C ₄₄ H ₄₆ I ₂ N ₄ Se ₂
Formula weight	1042.57
Temperature/K	150(2)
Crystal system	Triclinic
Space group	P-1
a/Å	7.7599(8)
b/Å	11.1126(9)
c/Å	24.7491(14)
α /°	82.510(6)
β /°	83.524(7)
γ /°	69.585(9)
Volume/Å ³	1977.9(3)
Z	2
$\rho_{\text{calc}}/\text{cm}^3$	1.751
μ/mm^{-1}	14.872
F(000)	1024
Radiation	CuK α ($\lambda = 1.54184$)
Index ranges	$-8 \leq h \leq 9, -12 \leq k \leq 13, -29 \leq l \leq 29$
Reflections collected	11736
Independent reflections	6908
Data/restraints/parameters	6908 /0/ 471
Goodness-of-fit on F ²	0.972

Final R indexes [$I \geq 2\sigma(I)$]	$R_1 = 0.0504$, $wR_2 = 0.1304$
Final R indexes [all data]	$R_1 = 0.0594$, $wR_2 = 0.1420$
CCDC No	2261160

References:

1. B. Liu, Y. Pang, R. Bouhenni, E. Duah, S. Paruchuri, L. McDonald, *Chemical Communications* 2015, **51**, 11060-11063.
2. (a) E. Herz, T. Marchincin, L. Connelly, D. Bonner, A. Burns, S. Switalski and U. Wiesner, *Journal of Fluorescence*, 2010, **20**, 67-72 ; (b) K. P. Divya, S. Savithri and A. Ajayaghosh, *Chemical Communications*, 2014, **50**, 6020-6022 ; (c) D. F. Eaton, *Pure and Applied Chemistry*, 1988, **60**, 1107-1114 ; (d) C. Würth, M. Grabolle, J. Pauli, M. Spieles and U. Resch-Genger, *Nature Protocols*, 2013, **8**, 1535-1550.
3. V. Rathore, A. Upadhyay and S. Kumar, *Organic Letters*, 2018, **20**, 6274-6278.
4. R. A. Balaguez, R. Krüger, C. S. Radatz, D. S. Rampon, E. J. Lenardão, P. H. Schneider and D. Alves, *Tetrahedron Lett*, 2015, **56**, 2735-2740.
5. I. C. Mondal, M. Galkin, S. Sharma, N. A. Murugan, D. A. Yushchenko, K. Girdhar, A. Karmakar, P. Mondal, P. Gaur and S. Ghosh, *Chemistry – An Asian Journal*, 2022, **17**, e202101281.
6. Crys AlisPro Program, ver. 171.37.33c. Data Collection and Processing Software for Agilent X-ray Diffractometers; Agilent Technologies: Oxford, UK, 2012, 1–49.
7. G. M. Sheldrick, SADABS. Program for Empirical Absorption Correction. University of Gottingen, Germany, 1996.
8. G. M. Sheldrick, Crystal structure refinement with *SHELXL*. *Acta Crystallogr.* 2015, *C71*, 3–8.
9. L. J. Farrugia, WinGX and ORTEP for Windows: an update. *J. Appl. Crystallogr.* 2012, **45**, 849–854.
10. A. Karmakar, M. M. A. Soliman, G. M. D. M. Rúbio, M. F. C. Guedes da Silva and A. J. L. Pombeiro, *Dalton T*, 2020, **49**, 8075-8085.